

RADIOLOGY MEDICAL IMAGE FUSION USING NEURAL NETWORK

Dudam Chandana*¹

*¹KL University, India.

DOI : <https://www.doi.org/10.56726/IRJMETS45033>

ABSTRACT

Image fusion plays a key role in combining data from many sources into a single, more intelligible result in a range of clinical applications. The use of a medical image fusion technology can be beneficial to aid the physician in performing combination Preoperative preparation, intra-operative supervision, and interventional treatment are all part of the diagnostic process. In this thesis, proposed a technique with a combined model of PCA and CNN for the fusion of images A real-time image fusion method that uses pre-trained neural networks to create one image using features from several sources in real-time. Based on deep neural network feature maps, using a convolutional network a unique technique is produced to merge the images. Due to the vast number of capture systems, picture fusion has become increasingly important in current image processing applications. Fusion of pictures is used to combine multi-temporal, multi-view, and inter-data into single imaging with improved image quality and important feature integrity retained It's a crucial stage in a range of applications, including human-robot interaction, aircraft, satellites, and medical imaging, as well as robotics and object tracking.

Keywords: PCA, CNN, Fusion, Medical Image-Fusion.

I. INTRODUCTION

Bringing two or more things together to make a single entity is the process known as fusion. Medical image fusion tries to extract as much valuable information as possible from source photos to improve the usage of medical images and assist physicians in understanding image content. The merged image has better detail and precision than any of the source photos. The technique of fusing two or more images into a sequence of images that integrates the data from the individual images is known as image fusion. In comparison to any of the input images, the outcome is an image with more information content. The goal of picture fusion is to create images that are more acceptable and intelligible for human and machine perception, not just to minimize the number of data X-rays, SPECT, MRI, positron emission tomography (PET), computed tomography (CT), and other imaging devices produce common medical images. Medical image fusion combines data from multiple input images of the same tissue to generate a series of images that is easier to understand. Obtaining more information from medical photos using a variety of techniques, the use of a medical image fusion technology can be beneficial assist the physician in performing combination diagnostic and interventional treatment in a variety of clinical applications. This method of medical fusing became a popular tool for diagnosing illnesses.

Deep learning has made significant progress in a variety of Issues in computer vision applications, such as identification, fragmentation, and extremely Deep learning-based research in the field of image fusion has been a popular issue in recent years. Thanks to the continuous advancement of medical tomography and knowledge processing technologies, pixel-based image fusion utilizing multimodal medical information for severe clinical analysis, multi-focus illustrations for digitalization, and remotely sensed pictures for concealed gun identification is now possible. Image fusion is the use of techniques to combine two or more separate images to create a new image. It extracts data enhancing the resolving power of the initial multi-spectral image while maintaining the spectrum information from multi-source photos. It produces a fresh output image that is better suited for human/machine identification or further processing in medical. The accuracy of picture-guided sickness analysis, diagnostics, and healthcare problem evaluation are improved by image fusion. Medical imaging, fingerprints, automated prediction, machine vision, navigational, armed services technologies, remote sensing, digital photography, airplanes and spaceship imaging, industrial automation, multifocal imaging, and micro image analysis are all examples of image fusion applications., professional imaging, and concealed weapon detection, to name a few. We investigate the case where there are only two modal source photos to choose from. To support multimodal (more than two) photo fusions, they can be expanded to a tri extracting features network. Minimizing MSE loss raises the objective assessment index, however, this does not guarantee

acceptable visual quality. We took a combination of MRI-CT, a combination of MRI-PET, a combination of MRI-SPECT.

A computed tomography scan often called a CT scan is a non-invasive surgical imaging technique implemented in radiology to obtain detailed interior images of the human body. Typical x-rays don't show your bone, muscles, or body tissues, as well as this picture, does. CT scans can reveal a tumor's shape, size, and location.

The medical imaging technique of magnetic resonance (MRI) is often used in radiography to capture things of the body's structure and physiology. MRI scanners use magnetism, strong magnetic variations, and radio waves to produce images of internal tissues. A magnetic resonance imaging (MRI) scan can reveal structural flaws acting against the nerves, allowing the issue to be resolved before permanent nerve damage occurs. Neural damage is normally diagnosed through neuropsychological tests, and MRI scan information can also be utilized to corroborate the diagnosis.

II. LITERATURE SURVEY

To boost image content, medical image fusion combined images from several imaging methods such as computerized tomography (CT), MRI, positron emission tomography (PET), and single-photon emitter computerized tomography. Image fusion aims to integrate more valuable information with sources register photographs while deleting redundant data.

Quantitative analysis is performed utilizing entropy, fusion factor, fusion-symmetric, and data fusion, and comparative analysis is performed based on all technique's merits and limitations. We used a combination of CT and MRI scans to conduct our analysis.

Liguo Zhang proposed a final deep learning model for extracting features, feature merging, and image for restoration that reduces the requirement for sophisticated feature matching and fusion rules to be developed manually. [1].

Rajalingam Balakrishnan suggested a deep learning convolution neural network (CNN)-based multimodal medical picture fusion approach for the fusion process. A weight map is built by a convolutional neural network that combines two or even more multimodality medical pictures from pixels data for the fusion process [2].

Ebenezer Daniel proposed an algorithm using new hybrid wolf optimization, homomorphic wavelet fusion was named optimal homomorphic wavelet fusion (OHWF) [3].

Rui Zhu proposes a different multi-modality medical image fusion technique (S-ADE) by focusing upon this Synchronized-Anisotropic Diffusion Equation. The modified S-ADE model is utilized first to deconstruct two sources [4].

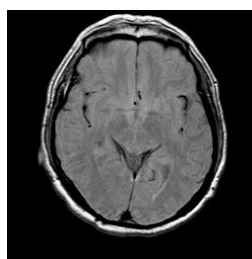
This model works best with MRI and CT scans. RenanNie presented medical photos of multimodal depend on the multi-information exchange encoding (MIEE) using a Pulse Coupled Neural Network (PCNN) by novel fusion architecture for [5].

A. P. Jamesa presents a detailed list of methodologies as well as a summary of the broad scientific issues that medical picture fusion faces. To tackle the ripple-II transform's shift variance problem, Hamid Reza Shahdoosti developed the dual ripple-II transform (DRT). The suggested approach uses the structural tensor and DRT to effectively combine the Medical Resonance Image and Positron emission tomography images. The proposed transform incorporates the dual-tree complex wavelet into the standard ripple-II transform. [6].

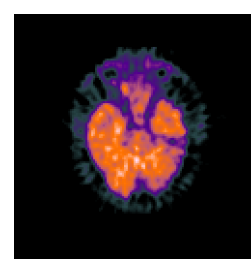
III. DATASET



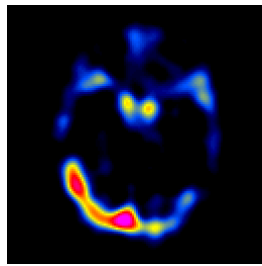
CT



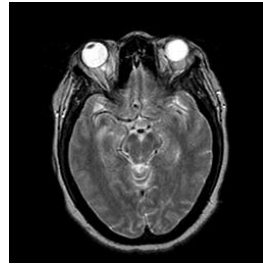
MRI



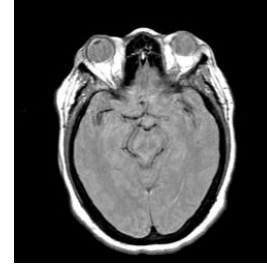
PET



SPECT



T1

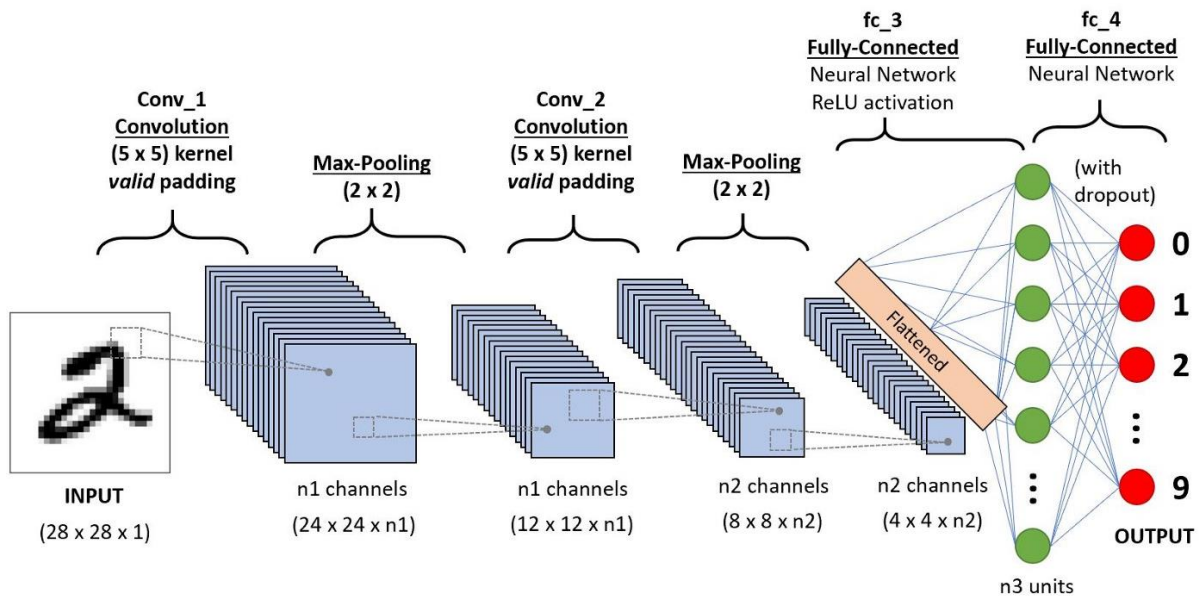


T2

IV. METHODOLOGY

4.1 Convolutional Neural Network

Convolutional networks, also known as convolutional neural networks, are neural network type that is utilized to process input with a specified grid-like architecture (LeCun, 1989). Convolutional networks have had a lot of success in real-world applications. The network's use of the convolutional mathematical procedure is a "convolutional neural network". It is a linear operation that is specialized. These networks are simple neural networks with a minimum of one layer that only uses convolution in the place of general matrix multiplication. Convolutional networks were among the first neural networks to solve key business problems, and they continue to be at the core of commercial deep learning applications today. A convolutional neural network consists of several layers which are classified as the Input layer, Convolutional layer, Max Pooling layer, flatten layer, Output layer which helps us to extract features and for the fusion of images. A tiny portion of the visual field reacts to stimuli in the Receptive Field which are known as neurons. A ring of comparable fields forms around the entire field of vision.



Deep Learning improvements in Machine Vision have been constructed and improved over time, mainly with the use of a single method the Convents.

4.1.2 VGG16

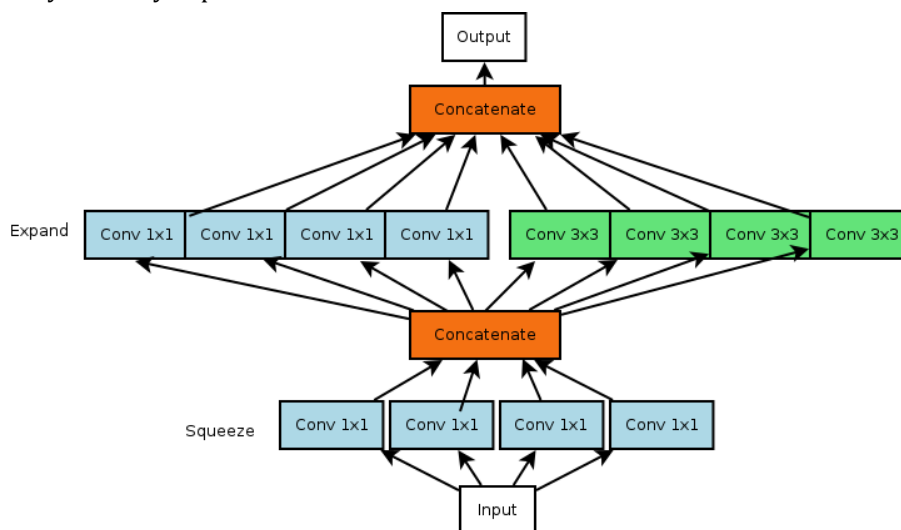
It is a deep Convolutional Neural (CNN) architecture with several layers. VGG means for Visual Geometry Group.VGG-16 is a deep convolutional neural network with 16 layers. It has a very appealing architecture due to its uniformity. It features only 3x3 convolutions, but a lot of filters, similar to AlexNet. It may be taught for two to three weeks on 4 GPUs. It is now the most popular method for extracting characteristics from photos in the community In ImageNet, The top-5 precision of the VGG16 model was 92.7 percent. The VGG16 Architecture was invented and presented by Karen Simonyan with Andrew Zisserman of Oxford University in their article "Very Fully Convolutional Networks for Large Object Recognition" in 2014.

4.1.3 VGG19

The VGG19 model is a VGG version with nineteen layers which is a combination of sixteen convolution layers, three fully linked layers, five max pool layers, and one SoftMax layer). The VGG19 (also known as VGGNet-19) is a model similar to VGG16 only it contains 19 layers. The weight layers of the model are represented by the digits "16" and "19". (convolutional layers). In comparison to VGG16, VGG19 has three more convolution layers. VGG19 is a complex CNN having pre-trained phases and a deep understanding of how a picture is described in terms of appearance, color, and structure. VGG19 is a neural network that was learned on millions of pictures to solve difficult classification issues. For a wide range of images, the system has learned rich feature representations.

4.1.4 SqueezeNet

Squeeze Net is an eighteen-layer deep convolutional neural network. SqueezeNet is a type of neural network that employs design strategies to reduce dimensionality, most notably by the use of flame components, which "squeeze" variables using 1x1 CNNs. The authors' purpose in developing SqueezeNet was to form a small neural net with fewer features that could fit into memory storage and be communicated over just a computer network more readily. SqueezeNet is a tiny network that was created to be a more compact alternative to AlexNet. It has over 50 times fewer parameters than AlexNet yet performs three times faster. The "squeeze" and "expand" layers make up the SqueezeNet architecture. Only one filter is used in a squeeze convolutional layer. These are sent through a mix of 1 1 and 3 3 convolution filters in an extended layer. SqueezeNet was trained at a learning algorithm of 0.04, which decreases linearly as the training progresses. Because of its modest size, SqueezeNet simplifies the setup procedure easier. This network was first built in Caffe but it has grown in prominence and has been adopted by a variety of platforms.



4.2 Principal Component Analysis

Principal Component Analysis is indeed an unsupervised learning approach is implemented in machine learning to reduce dimensionality. It is a mathematical strategy that transforms outputs of correlated attributes into a collection of uncorrelated characteristics which are linear by using orthogonal information. The newly revised characteristics are the Principal Components.

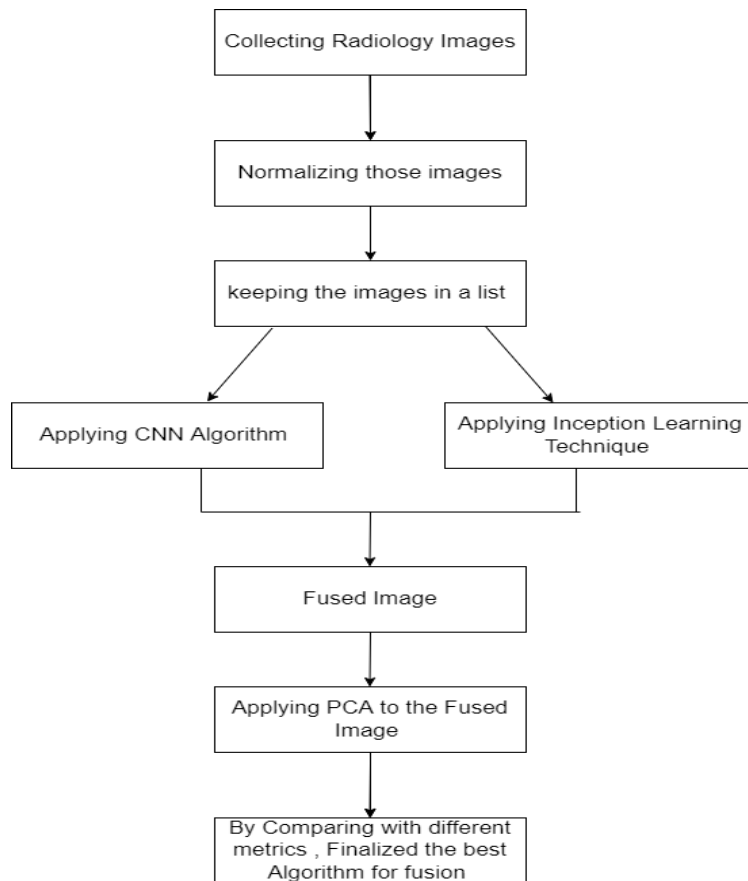
The principal component analysis is a method for condensing a large set of samples into a smaller set that retains the bulk of the data from the bigger set. The principal component analysis technique allows us to build and use a smaller collection of variables known as primary factors. It's considerably easier to study and interpret a smaller set. The fusion of images from a regular video and an infrared sensor is presented in this study.

4.3 Proposed model

Firstly, radiology images were collected and followed by normalization, that improves both the efficiency of computation and better execution. Later those normalized images were given to CNN algorithm for fusion process and finally fused images are collected and sent to PCA algorithm for dimensionality reduction. This

made the technique as combine model of CNN +PCA which gives better results than other algorithms. For verifying the accuracy of other algorithms for fusion of images, the normalised image is sent to VGG16, VGG19, Squeeze net and PCA but the results that observed are less accurate than the combine model of CNN+PCA. Here for the fusion of images, collected various model of radiology pictures such as MRI, CT, PET, SPECT. For this image fusion two different format images are taken like MRI: CT, MRI: PET, MRI: SPECT.

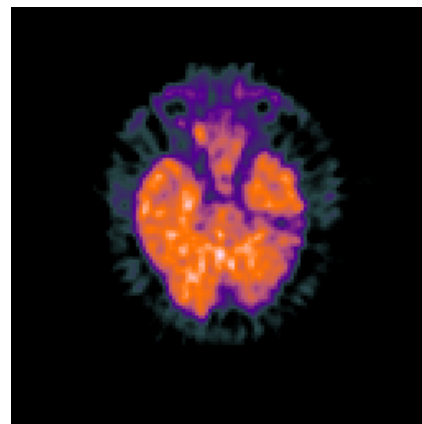
FLOW CHART



I PET-MRI



(a) MRI



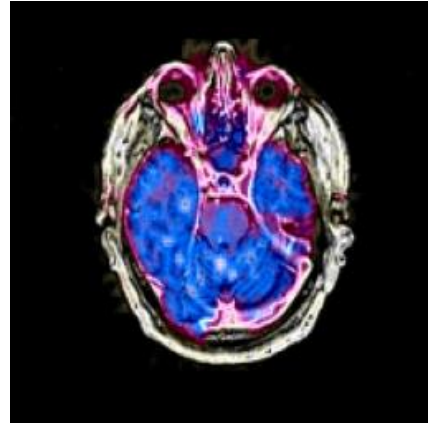
(b) PET

The Source images are taken from the regular brain in different radiology techniques. The real brain of MRI and PET input images are gathered for a source for testing, and the fuse output is produced again by integrating its inverted output of the resultant connection with actual U & V segments. Implementation of the algorithm is simple for source images; however, the fusion outcome is not perfect. The fusion image is not stable because the information of the fused image is changing from one algorithm method to another algorithm method, but the data image consists of different modalities concerning the algorithm used. Compare to other fused images

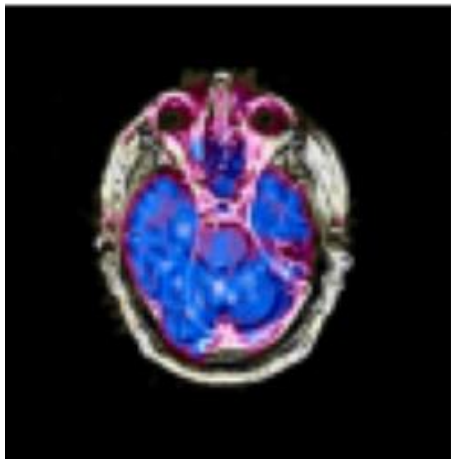
the PCA image color changes. While in PCA the obtained fused image will be in the grayscale mode because we are not converting the mode of a fused image. So, the better-fused image is observed for CNN + PCA.



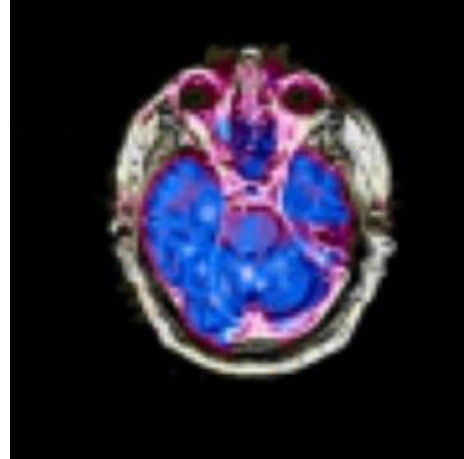
(c) PCA



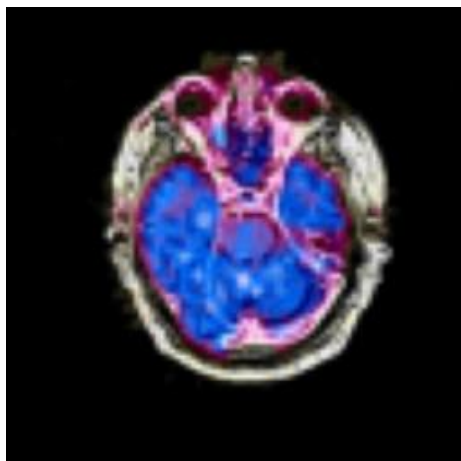
(d) Squeeze Net



(e) VGG-16

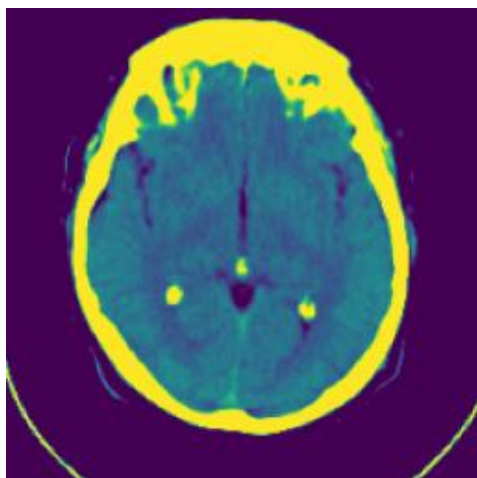


(f) VGG-19

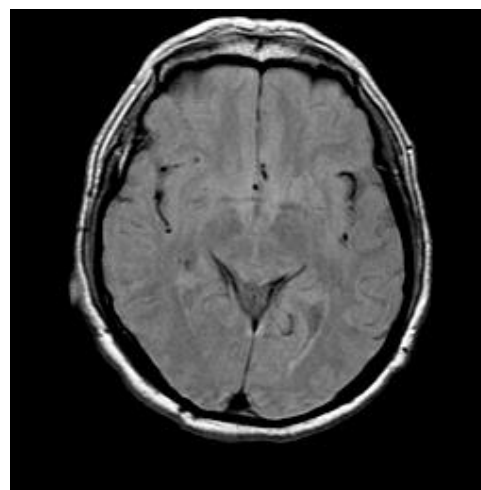


(g) CNN+PCA

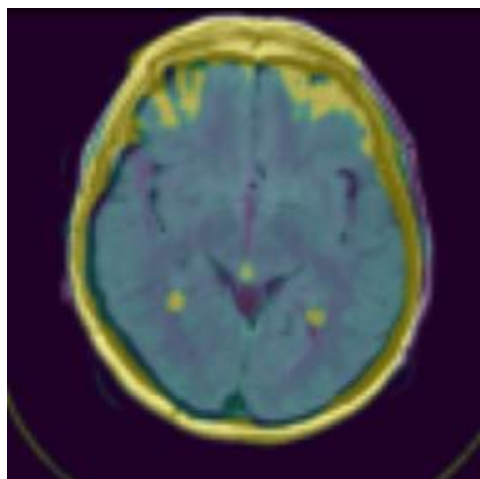
II MRI-CT



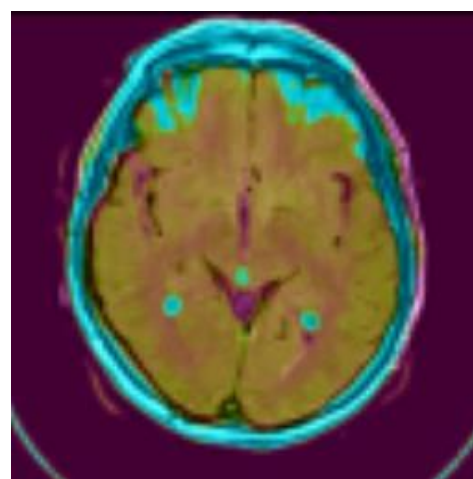
(a) CT



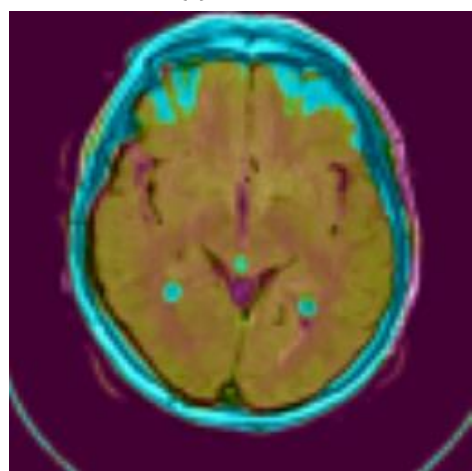
(b) MRI



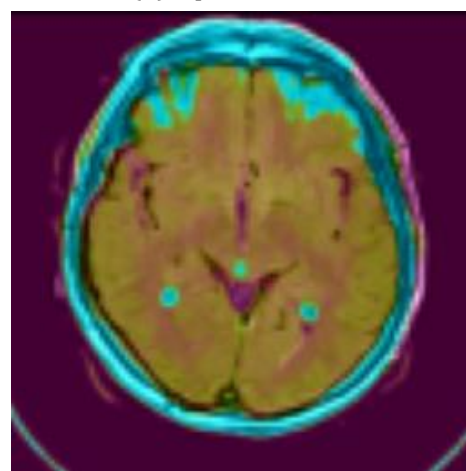
(c) PCA



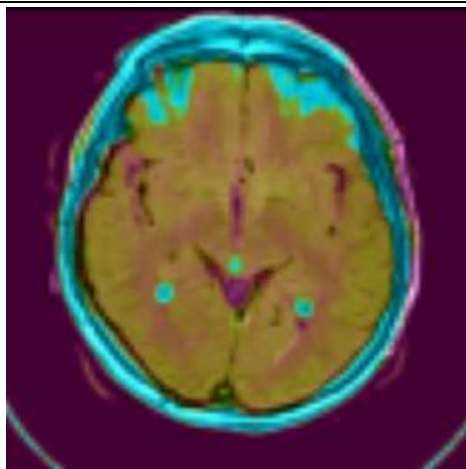
(d) SqueezeNet



(e) VGG-16

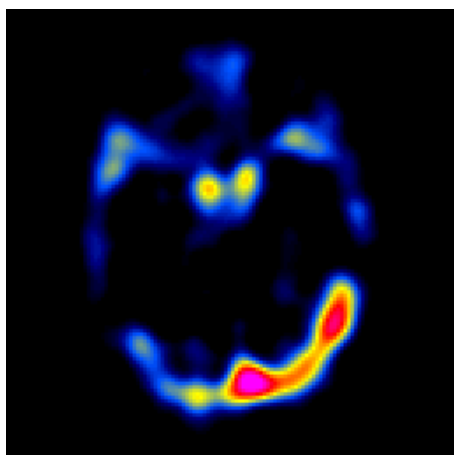


(f) VGG-19

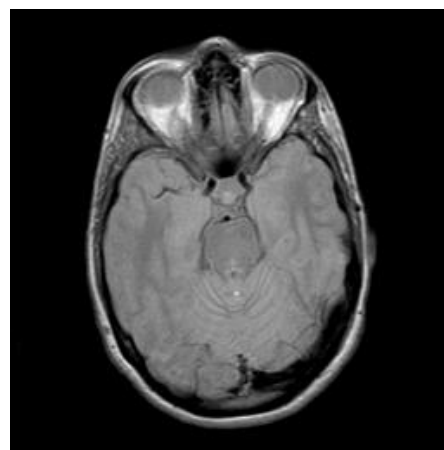


(g) CNN+PCA

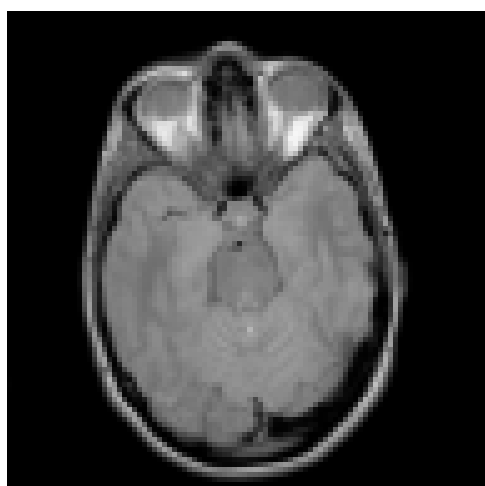
III MRI-SPECT



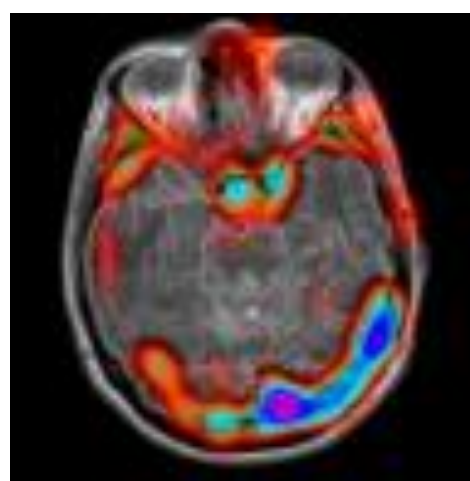
(a) SPECT



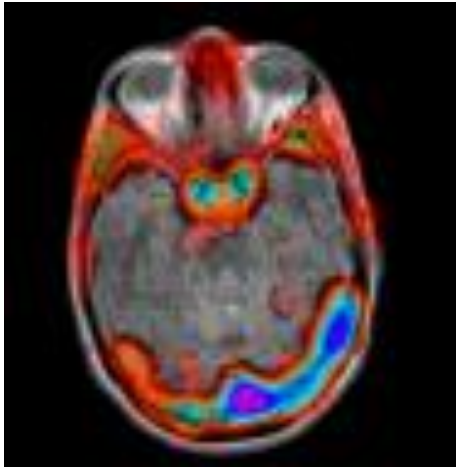
(b) MRI



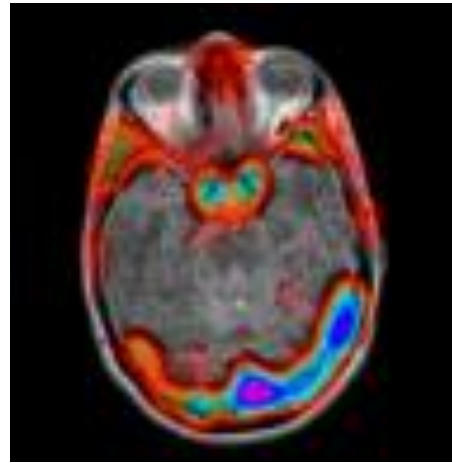
(c) PCA



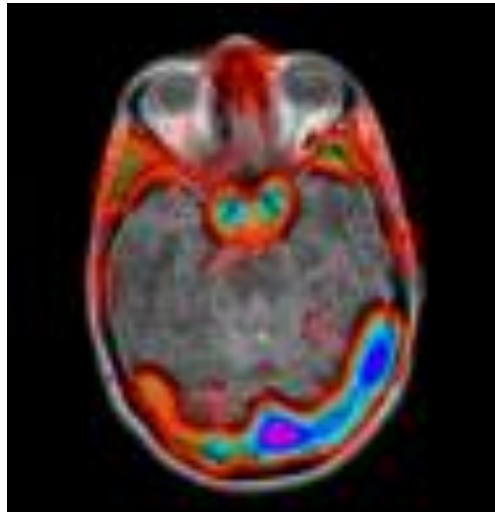
(d) Squeeze Net



(e) VGG-16

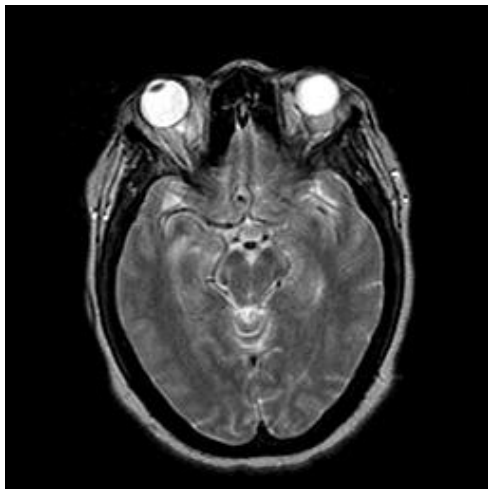


(f) VGG-19

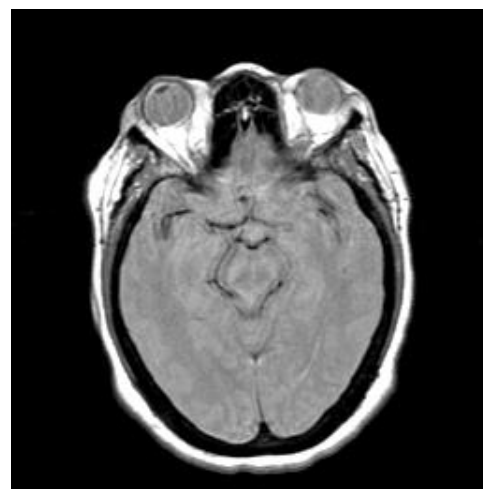


(g) CNN+PCA

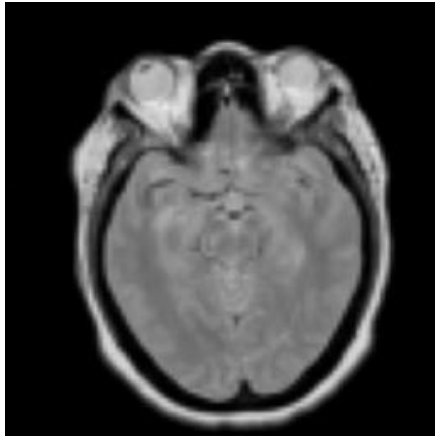
IV T1-T2



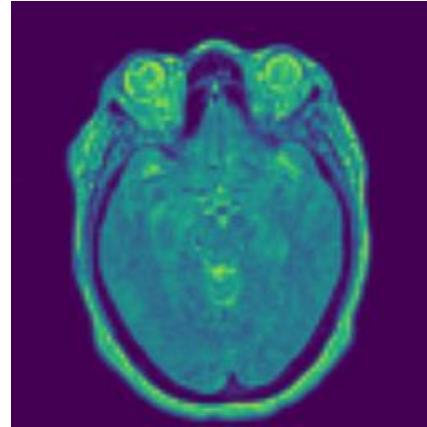
(a) MRI-T1



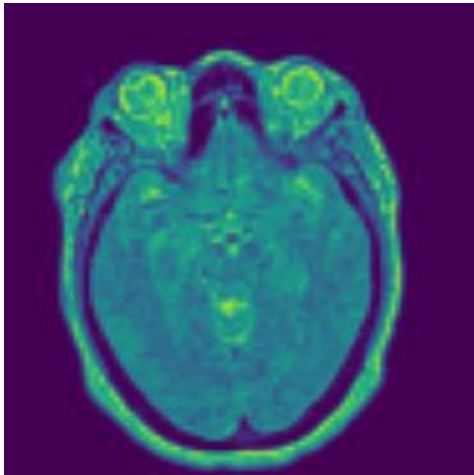
(b) MRI-T2



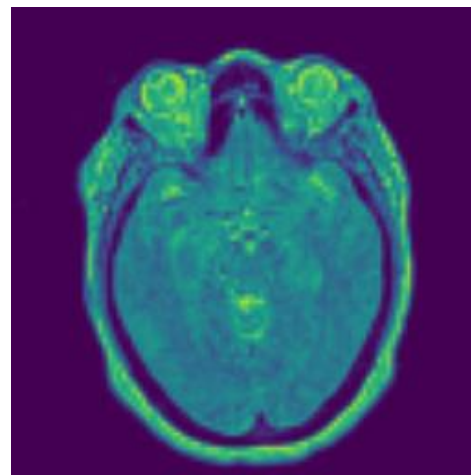
(c) PCA



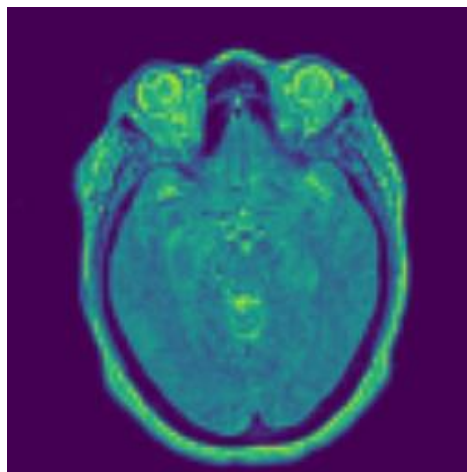
(d) Squeeze Net



(e) VGG-16



(f) VGG-19



(g) CNN+PCA

In I, II, III, IV, they are source images and fused images using different algorithms. The images are having different modalities with the size of 256*256 pixels. The PCA fused image is obtained with the help of reshaping, eigenvectors, and eigenvalue, the fused image is in grey mode. From the above figures, the information is more plentiful, with higher-rated visual quality for CNN+PCA.

V. RESULT AND DISCUSSION

In this section, we will discuss the comparative analysis of different algorithm methods using various metric indexes with the help of the programming language Python. Then the obtained result uses the proposed algorithm among the algorithm's method and selects the best algorithm method.

The comparative analysis is based on source images and fused image with help of comparing algorithm methods including the add-weighted average of them.

5.1 Results:

As earlier mentioned, the fused images were created utilizing several methods such as VGG-16, VGG-19, Squeeze Net, PCA, and CNN+PCA.

5.2 Metric Indexes

How to accurately evaluate the efficiency of fusion methods is an essential topic in picture fusion. In recent years, several other assessment indexes have been proposed. There are two types of assessment methods now in use: the quality evaluation using a source image and a non-source image. Evaluation of image quality, we choose five metrics, for the accurate understanding of their outcomes: Mean Square Error (MSE) be a part of the objective evaluation index that must be consulted the Structural Similarity Index (SSIM), Information Entropy (EN), Normalized Mutual Information (Qmi) and visual information fidelity (VIF) pixel, all of which are objective evaluation indicators. There is no need for reference images.

5.2.1 MSE: The mean-square error (MSE) is a measure that depicts the radiometric variations between fusion results on a global scale. The value shows the overall variation between the proposed method fusion outcome image as well as fusion image.

G(i, j)= genuine image

F(i, j) = fused image is labeled

m & n = the record number of source image height & width

$$MSE = \frac{\sum_{j=1}^N \sum_{k=1}^M (F(j, k) - G(j, k))^2}{n \times m}$$

5.2.2 SSIM: The Structural Similarity Index (SSIM) has the performance indicator of how similar 2 images are. The following is its definition:

$$SSIM(a,b) = \frac{(2\mu_a\mu_b + d_1) (2\sigma_{ab} + d_2)}{(\mu_a^2 + \mu_b^2 + d_1)(\sigma_a^2 + \sigma_b^2 + d_2)}$$

a = algorithm's fusion image

b = true image

μ_a, μ_b = average of (a, b)

σ_a^2, σ_b^2 = variances of (a, b)

σ_{ab} = covariance (a,b).

d_1, d_2 = aid in the stability of the situation

5.2.3 VIF: Visual Information Fidelity (VIF) is the parameter for evaluating image quality that is based on information aspects of natural scenes statistical (NSS).

$$VIF(x, y) = \frac{\sum_{k=1}^s \sum_{i=1}^{M_k} A(p_{i,k}, r_{i,k})}{\sum_{k=1}^s \sum_{i=1}^{M_k} A(p_{i,k}, q_{i,k})}$$

$A(p_{i,k}, q_{i,k})$ = actual image details

$A(p_{i,k}, r_{i,k})$ = unbalanced image details

$p_{i,k}, q_{i,k}$ and $r_{i,k}$ = p, q, and r in images frames in a variety of sizes

M_k = scale's amount of image pixels k

s = the variety of categories in which the image is split

5.2.4 Entropy: The expected value along with the random variable is measured using entropy. The image's color histogram can be thought of as a probability density function.

The detailed entropy of a picture is represented with h(i) where h(i) reflects the quantized color's % of pixel i in the overall image.

$$Entropy = \sum_{i=1}^n h(i) \log_2 h(i)$$

5.2.5 Mutual Information: Q_{MI} (Normalized Mutual Information) measures the degree of collaboration between the image of the output and the visual of the input. This demonstrates the similarity of the source and merged images. The normalized mutual information Q_{MI} expression is as follows:

$$Q_{MI} = 2 \left[\frac{MI(C, R)}{Q(C) + Q(R)} + \frac{MI(D, R)}{Q(D) + Q(R)} \right]$$

Mutual Information (MI) could be a statistical estimate on 2 variables that is interconnectedness will occur directly using {Equation MI (U, V)} H(C), H(D), and H(R) are entropies that can be obtained using H(U) formula.

$$MI(U, V) = \sum_{v \in V} \sum_{u \in U} g(u, v) \log_2 \frac{g(u, v)}{g(u)g(v)}$$

$$Q(U) = \sum_{u \in U} g(u) \log_2 g(u)$$

5.3 Performance Evaluation

In this experiment, we have selected a few pairs of radiology medical images as the test data. For test data, we have applied filters for better understanding. The comparing algorithms are based on VGG-16, VGG-19, SQUEEZENET, Principal Component Analysis (PCA), and CNN+PCA. Among them, we randomly choose two source images with diverse modalities. The input image is transformed from RGB to HSI space at the time of testing, and various another format like grayscale, YCbCr, gray, etc.

A metric score of fusion methods:

TABLE 1: MRI-PET Metric Score

	VGG-16	VGG-19	SQUEEZE NET	PCA	CNN+PCA
MSE	3821.896868	4326.268603	5248.530215	3795.749468	3841.147947
SSIM	0.634070678	0.599964187	0.576918209	0.593477189	0.631366731
VIF	0.020115451	0.026862346	0.017607955	0.022060916	0.082619463
Entropy	3.770389411	4.070330749	4.112055998	3.990689894	3.001083163
MI	0.436537877	0.435251605	0.371655424	0.467336177	1.145331026

TABLE 2: MRI-CT Metric Score

	VGG-16	VGG-19	SQUEEZE NET	PCA	CNN+PCA
MSE	5256.273155	4616.454714	5309.027707	22221.134702	20859.81113
SSIM	0.338170304	0.373294043	0.353296692	0.428951084	0.060058943
VIF	0.03505622	0.053515519	0.045902515	0.078706307	0.015024352
Entropy	6.420616688	6.279529215	6.173356001	5.989346358	4.957725674
MI	0.658167886	0.724539243	0.718558411	0.878390975	1.265098822

TABLE 3: MRI-SPECT Metric Score

	VGG-16	VGG-19	SQUEEZE NET	PCA	CNN+PCA
MSE	4271.68407	4227.611837	4556.879791	3455.778519	5779.010585
SSIM	0.486359572	0.473912872	0.470555961	0.591496644	0.48038565
VIF	0.047101677	0.044480608	0.037290363	0.107424537	0.048830219
Entropy	4.729863707	4.815029541	4.693647639	4.380235834	3.202091852
MI	0.362361713	0.324649206	0.308850748	0.586975232	1.573748002

TABLE 4: MRT1- MRT2 Metric Score

	VGG-16	VGG-19	SQUEEZE NET	PCA	CNN+PCA
MSE	5178.371531	5417.560435	3095.919525	2668.707336	4735.199752
SSIM	0.17952148	0.167316343	0.478195945	0.515009571	0.4094382486
VIF	0.031350142	0.024646476	0.062285785	0.075168443	0.0615285748
Entropy	5.695356778	5.763374805	5.290079636	5.277351219	3.9653502677
MI	0.493445079	0.459940614	0.531062598	0.626701992	1.119491017

In the above TABLEs, the following are credible depictions of fused images created utilizing several ways of fusion: Mean Square Error (MSE), Structural Similarity Index (SSIM), Information Entropy (EN), Normalized Mutual Information (Q_{MI}) Normalized Mutual Information based on identical, and Visual Information Fidelity (VIF) based on pixel-image. The per average for every metric of source images to fused images is provided in the table. The proposed metric result is CNN+PCA. In MSE, with the rise of the metric score, the performance of source images and fusion images is better. And the higher VIF metric score, indicates the better the image quality i.e., fused image. From the tables of MRI-CT, MRI-PET, MRI-SPECT, we can observe that the proposed method which is in bold font performance is better than the other algorithm methods. Finally, we compared the metric scores for different algorithm methods. The source images with different modalities with a size of 256*256 pixels. The proposed method is implemented in python with the help of a torch tool for different neural networks. The python version takes less time to accomplish the fusion.

VI. CONCLUSION

The method extracts further information from source images using weights that are not shared. CNN is used with PCA in the proposed method for image reconstruction, and it also aids during lowering the computational complexity and dimensionality of the original pictures. MSE loss is the basis for the proposed method loss function. Minimizing MSE loss raises the objective assessment index, however, this does not guarantee acceptable image fidelity. Its focus on the future discussion will be refining the loss function as well as enhancing its effectiveness images that were fused to get a bunch more durable fusion method according to CNN. The proposed model's fusion image can effectively fully preserve the useful information in the source images possible. The proposed method outperforms other comparison methods in terms of evaluating image fusion metrics. The proposed method is stable in terms of durability and may be applied to image fusion.

ACKNOWLEDGEMENTS

The author express sincere gratitude to the Koneru Lakshmaiah Education Foundation for supporting this work, The author would also like to thank the:

1. "The Whole brain Atlas" (<https://www.med.harvard.edu/aanlib/>).
2. "Kaggle dataset" for the source images.

VII. REFERENCE

- [1] X. Liang, P. Hu, L. Zhang, J. Sun and G. Yin, "MCFNet: Multi-Layer Concatenation Fusion Network for Medical Images Fusion," in IEEE Sensors Journal, vol. 19, no. 16, pp. 7107-7119, 15 Aug.15, 2019, DOI: 10.1109/JSEN.2019.2913281.
- [2] https://www.researchgate.net/publication/326913625_Multimodal_Medical_Image_Fusion_based_on_Deep_Learning_Neural_Network_for_Clinical_Treatment_Analysis
- [3] E. Daniel, "Optimum Wavelet-Based Homomorphic Medical Image Fusion Using Hybrid Genetic-Grey Wolf Optimization Algorithm," in IEEE Sensors Journal, vol. 18, no. 16, pp. 6804-6811, 15 Aug.15, 2018, DOI: 10.1109/JSEN.2018.2822712.
- [4] R. Zhu, X. Li, X. Zhang, and M. Ma, "MRI and CT Medical Image Fusion Based on Synchronized-Anisotropic Diffusion Model," in IEEE Access, vol. 8, pp. 91336-91350, 2020, DOI: 10.1109/ACCESS.2020.2993493.
- [5] R. Nie, J. Cao, D. Zhou, and W. Qian, "Multi-Source Information Exchange Encoding With PCNN for Medical Image Fusion," in IEEE Transactions on Circuits and Systems for Video Technology, vol. 31, no. 3, pp. 986-1000, March 2021, DOI: 10.1109/TCSVT.2020.2998696.

- [6] A. P. James and B. V. Dasarathy, "Medical image fusion: A survey of the state of the art", *Inf. Fusion*, vol. 19, pp. 4-19, Sep. 2014.
- [7] A. Galande and R. Patil, "The art of medical image fusion: A survey," 2013 International Conference on Advances in Computing, Communications and Informatics (ICACCI), 2013, pp. 400-405, doi: 10.1109/ICACCI.2013.6637205.
- [8] B. Ashwanth and K. V. Swamy, "Medical Image Fusion using Transform Techniques," 2020 5th International Conference on Devices, Circuits and Systems (ICDCS), 2020, pp. 303-306, doi: 10.1109/ICDCS48716.2020.243604.
- [9] P. Prasad, S. Subramani, V. Bhavana and H. K. Krishnappa, "Medical Image Fusion Techniques Using Discrete Wavelet Transform," 2019 3rd International Conference on Computing Methodologies and Communication (ICCMC), 2019, pp. 614-618, doi: 10.1109/ICCMC.2019.8819672.
- [10] B. Pal, S. Mahajan and S. Jain, "Medical Image Fusion Employing Enhancement Techniques," 2020 IEEE International Women in Engineering (WIE) Conference on Electrical and Computer Engineering (WIECON-ECE), 2020, pp. 223-226, doi: 10.1109/WIECON-ECE52138.2020.9398021.
- [11] H. M. El-Hoseny, E. M. El Rabaie, W. A. Elrahman and F. E. Abd El-Samie, "Medical image fusion techniques based on combined discrete transform domains," 2017 34th National Radio Science Conference (NRSC), 2017, pp. 471-480, doi: 10.1109/NRSC.2017.7893518.
- [12] N. George and K. K. Saju, "Study on Image Fusion Techniques Applicable to Medical Diagnosis," 2018 International Conference on Emerging Trends and Innovations In Engineering And Technological Research (ICETIETR), 2018, pp. 1-5, doi: 10.1109/ICETIETR.2018.8529062.
- [13] Y. Liu, X. Chen, J. Cheng and H. Peng, "A medical image fusion method based on convolutional neural networks," 2017 20th International Conference on Information Fusion (Fusion), 2017, pp. 1-7, doi: 10.23919/ICIF.2017.8009769.
- [14] S. Polinati and R. Dhuli, "A Review on Multi-Model Medical Image Fusion," 2019 International Conference on Communication and Signal Processing (ICCSP), 2019, pp. 0554-0558, doi: 10.1109/ICCSP.2019.8697906.
- [15] J. M. Dolly and N. A.K., "A Survey on Different Multimodal Medical Image Fusion Techniques and Methods," 2019 1st International Conference on Innovations in Information and Communication Technology (ICIICT), 2019, pp. 1-5, doi: 10.1109/ICIICT1.2019.8741445.
- [16] J. Huang, Y. Wei and D. Liang, "A Deep Neural Network for Fusion with Medical Image Pair," 2021 IEEE 2nd International Conference on Information Technology, Big Data and Artificial Intelligence (ICIBA), 2021, pp. 553-557, doi: 10.1109/ICIBA52610.2021.9688075.
- [17] F. Lahoud and S. Süssstrunk, "Zero-Learning Fast Medical Image Fusion," 2019 22th International Conference on Information Fusion (FUSION), 2019, pp. 1-8.
- [18] M. Balpande and U. Shrawankar, "Medical image fusion techniques for remote surgery," 2013 Annual IEEE India Conference (INDICON), 2013, pp. 1-6, doi: 10.1109/INDCON.2013.6726108.
- [19] P. -W. Huang, C. -I. Chen, Ping Chen, P. -L. Lin and Li-Pin Hsu, "PET and MRI brain image fusion using wavelet transform with structural information adjustment and spectral information patching," 2014 IEEE International Symposium on Bioelectronics and Bioinformatics (IEEE ISBB 2014), 2014, pp. 1-4, doi: 10.1109/ISBB.2014.6820901.
- [20] M. P., T. Singh, R. Nayar and S. Kumar, "Multi Modal Medical Image Fusion using Convolution Neural Network," 2019 Third International Conference on Inventive Systems and Control (ICISC), 2019, pp. 351-357, doi: 10.1109/ICISC44355.2019.9036373.
- [21] Z. Le, J. Huang, F. Fan, X. Tian and J. Ma, "A Generative Adversarial Network For Medical Image Fusion," 2020 IEEE International Conference on Image Processing (ICIP), 2020, pp. 370-374, doi: 10.1109/ICIP40778.2020.9191089.
- [22] H. Zhang, L. Liu and N. Lin, "A Novel Wavelet Medical Image Fusion Method," 2007 International Conference on Multimedia and Ubiquitous Engineering (MUE'07), 2007, pp. 548-553, doi: 10.1109/MUE.2007.40.